

Development of an Upper Limb Exoskeleton Powered via Pneumatic Electric Hybrid Actuators with Bowden Cable

Tomoyuki Noda, Tatsuya Teramae, Barkan Ugurlu, and Jun Morimoto

Abstract—In this paper, we introduce our ongoing work on the development of an upper body exoskeleton robot, driven by a pneumatic-electric hybrid actuation system. Since the limb of an exoskeleton robot needs to have small inertia to achieve agility and safety, using a heavy actuator is not preferable. Furthermore, we need to use backdrivable actuators that can generate sufficiently large torques to support user movements. These two requirements may seem contradictory. In order to cope with this development problem, we use a hybrid actuation system composed of Pneumatic Artificial Muscles (PAMs) and small-size electromagnetic motors. Although we and other research groups have already presented the advantage of the hybrid actuation system, we newly propose the usage of Bowden cable in a hybrid actuator to transmit the force generated by the PAMs to joints of our exoskeleton robot so that we can design a compact upper limb with small inertia. In addition, small size electric motors are mechanically connected to joints in order to compensate uncertainty generated by the PAM dynamics and the Bowden cable. We demonstrate that the proposed joint is backdrivable with the capability of large torque generation for the gravity compensation task both in One-DOF system with a dummy weight and right arm of the upper body exoskeleton with a mannequin arm. We also show the right arm exoskeleton can be moved using a torque input, extracted from sensory information via a goniometer.

I. INTRODUCTION

Development of exoskeleton robots is an important research topic [1], [2] because such systems can be used to assist movements in supporting elderly people and can be a useful device for rehabilitation to help recovery of stroke patients or spinal cord injury patients [3]–[7].

Since an exoskeleton robot needs to simultaneously support the user's body weight and the weight of the robot itself, the limbs of the exoskeleton robot need to have small inertia but actuators need to be sufficiently strong. To satisfy these requirements, using Bowden cables to transmit forces generated by actuators, where the actuators are located apart from limbs of a robot, were proposed in several studies [8]–[13].

In this paper, we introduce our exoskeleton development for upper limbs with Bowden cables that transmit forces generated by actuators to joints of the robot. As the actuator system, we use pneumatic-electric hybrid actuators that we have been developing in our previous studies [14]–[17] but with PAMs force/displacement transmitted via Bowden cables in this paper. Pneumatic-Electric Hybrid Actuator (PEHA) is composed of a pair of Pneumatic Artificial Muscles (PAMs) and a small-size electromagnetic motor, where the PAMs can

be used to generate large and low frequency forces, and the small-size electric motor can generate additional small but high frequency torque. Since the developed exoskeleton robot has force sensors at the tip of each PAM, joint torques can be measured. In this study, we also introduce a model and a calibration method to explicitly consider force loss and wire extension when the force generated by the PAM is transmitted via Bowden cable while conventional studies neglected these significant problems by assuming that inner wires are infinitely stiff.

We demonstrate the superiority of the joint powered via PEHA with Bowden cables using the implemented controller: backdrivability, and possessing the capability of large torque generation. The practical calibration is also described. For proof of concept evaluation, we use the prototyped exoskeleton arm to compensate the gravitational force. (See the multimedia attachment.) To start with, we show One-DOF testing system that can be moved up and down by a finger. Similarly, the exoskeleton right arm demonstrates sustaining the mannequin arm with a passive elbow joint at different postures using exoskeleton's gravity compensated shoulder and active elbow joints.

The rest of the paper organized as follows. Section II describes the hardware design concept using the basic One-DOF PEHA architecture with/without Bowden Cable transmission system and discusses control problems with comparison of conventional researches. Section III describes mechatronics design, especially related to PAMs with Bowden Cable force transmission system. The upper body arm exoskeleton is prototyped in this section. Section IV considers a torque generation model, concerning the PAM with compensation for friction in Bowden cable to provide a torque controller which is calibrated in the system identification phase. Section V validates our design concept, using the upper right limb exoskeleton, both for a gravity compensation as passive movement and a torque input converted using a sensory information via subject's elbow goniometer as active movement. See also the multimedia attachment of this paper, demonstrating these tasks visually. We finally conclude in Section VI.

II. CONCEPT AND DESIGN POLICY

A. Actuator design and Torque Control Problem

1) *PEHA One-DOF system*: Fig. 1 shows the basic design of the PEHA One-DOF system. The paired PAMs generate antagonistic contraction force, transmitted via wires. The total torque, τ , is the sum of torques generated by PAMs

The authors are with Dept. of Brain Robot Interface, ATR Computational Neuroscience Labs, 2-2-2 Hikaridai, Seikacho, Souraku-gun, Kyoto, Japan, 619-0288 E-mail: {t.noda,t.teramae,barkanu,xmorimo}@atr.jp

for upper direction and 10mm for lower direction). The peak torques are 100 Nm at the shoulder and 76 Nm at the elbow without the Bowden cable coefficient. Nominal maximum forces of a 40mm PAM is 5000 N but limited up to 2000 N in this paper (see later subsection III-B). Nominal maximum force of 10mm PAM is 630 N as the antagonistic muscle for SFE and EFE. The motor (Maxon inc., EC-4pole 30 100W with low reduction gear (14:1) and a built-in optical quadrature encoder) torque is additionally delivered through the bevel gear (2:5). The nominal torque is approximately 2.5 Nm (maximum continuous without the gear coefficient). For WFE, 10mm PAMs are used for both directions without any motor to make the arm tip light, as already discussed above. Note that although the joint is backdrivable with small inertia thanks to the low gear reduction (35:1), the motor torque is not enough to sustain user's arm at all. PAM torque could be sufficiently large but its response is slow and prone to modeling errors. The combination of both PAM and motor torques is reasonable for the target tasks concerning gravity compensation for the robot and user arm.

Fig. 5 (a) shows the prototyped right arm and the overview of the case that the user arm is attached to the upper body exoskeleton arm. To connect the exoskeleton to the user's arm, the belts at the link both in Elbow–Wrist and Shoulder–Elbow can be installed. The total weight from shoulder to tip was within 5 kg, excluding controller units.

A. Controller Unit

Fig. 5 (b) and Fig. 5 (c) show the controller unit which is mechanically independent from exoskeleton arm structure, but connected via Bowden cable and electric cables. Fig. 5 (b) shows the mechanism to prevent loosening of inner wires by a passive movement at the pulley side. As the shoulder angle decreases, the inner wire pushes down itself toward the PAM side. The PAM is always required to control not to loosen wire, otherwise the wire may be buckled and come off from the pulley nest. The illustrated structure to prevent loosening of wire to below, avoiding the interference to the PAM edge. To our best knowledge, this problem was unconsidered in conventional research. Fig. 5 (c) illustrates the alignment of PAMs and valves. The multifunction board (MFB) and load cell amplifier are also located beneath motor drivers. MFB has 16bit 16ch AD, 16bit 8ch DA, 8bit IO, and 8ch of quadrature decoder for joint encoder. All the I/O pins of the system goes through the MFB communicating with realtime system (Xenomai PC) using Ethernet (RTnet UDP protocol, see also Fig. 3 (b))

B. Maximum Allowable PAM Force Determination and safety

Having very large power-to-weight ratios, the specific PAMs utilized in our exoskeleton arm are capable of producing forces up to 5000 [N]. On the contrary, Bowden cables or wire stoppers may not be operable when they are subject to such large forces. Keeping this in mind, a series of tests are conducted in which a single muscle is placed to an aluminum frame and mechanically connected to a fixed pulley via a

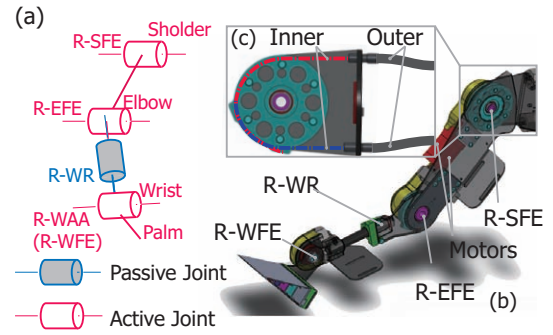


Fig. 4. The kinematic structure and the 3D CAD assembly of right arm exoskeleton prototype: (a) Kinematic model: Each abbreviation is [FE: Flexion Extension]; [AA: Adduction Abduction]; [R: Rotation]; [S: Shoulder]; [E: Elbow]; and [W: Wrist]. Before hyphenation, [R: Right] and [L: Left] indicate the side respect to user's view point. For example, R-SFE denotes the right shoulder Flexion Extension. (b) Agonist/Antagonist inner cables driven by two differential PAMs are connected to the joint pulley.

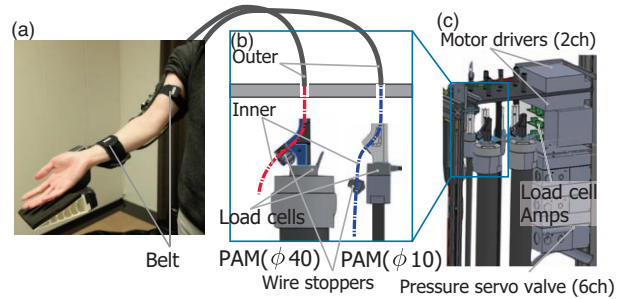


Fig. 5. Prototyped exoskeleton right arm and the controller unit: (a) The arm exoskeleton are attached to a human right arm. (b) The antagonistic pair of inner cables comes from the pulley side throughout the outer. The diameters, ϕ , are 40mm for agonist and 10mm for antagonist directions of shoulder and elbow joint. 10mm for agonist/antagonist direction of wrist. (c) Controller unit includes PAMs and pneumatic valves, located apart from the exoskeleton's kinematics, are to be mounted on a wheel chair or a weight bearing system. Motor drivers and load cell amplifier are also mounted in the control unit.

Bowden cable and a stopper. Fig.6 displays this setup and its elements. The diameter of the inner wire was 1.7 mm.

Subsequently, the muscle is activated with gradually increasing ramp inputs in a way to determine the force value at which the cable or stopper breaks. Fig. 7 shows load cell measurements from 4 consecutive experiments with different initial tension values. As may be observed in Fig. 7, the system is safely operable until 2250 [N]. Beyond this range, inner bowden cable (not the stopper) is broken. Considering an 11% of safety margin, it is determined that 2000 [N] is the maximum allowable PAM force; the controllers are programmed in a way not to produce forces larger than this limit. This limitation may be increased by replacing thicker Bowden cable, and we can also use thinner cables to limit force mechanically.

IV. METHOD: TORQUE BASED CONTROLLER

The torque controller for a joint driven by multiple torque sources has to solve the redundant solution. In this paper, we consider only the PAM force control toward upper direction, e.g., supposed; antagonistic muscle desired force is constant

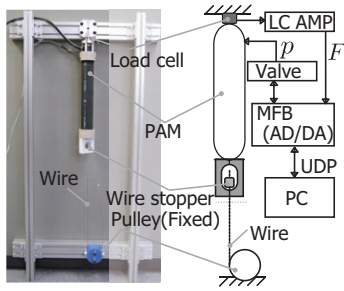


Fig. 6. Wire stopper experiment and block diagram of the experiment system.

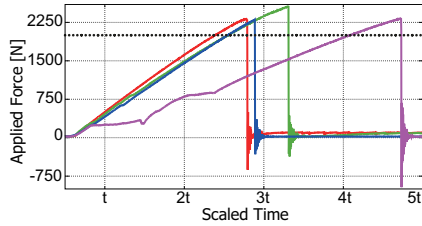


Fig. 7. Wire stopper evaluation: To evaluate the maximum allowable force to inner cable and the stopper, we applied tension using one PAM gradually from 4 different initial length.

and compliance of joint is subject to this constraint. For example, movement of the arm upper direction, desired antagonistic muscle force (f_{PAM2}^*) is controlled as constant; the simpler case 0[N]. In this case, the torque control problem becomes one PAM pressure control.

This simplified problem is still non-trivial. Primarily, PAM force is highly nonlinear [21] caused by its contraction rate. What is more, the operation in large force causes considerable cable extension between the encoder and PAM, resulting in the estimation error of PAM contraction rate. Secondly, the conventional researches [8]–[13] does not explicitly consider force losses between outer and inner in Bowden cable transmission system.

The force generation principle of PAM is that the bladder radial expansion causes the thrust contraction of wire surrounded or embedded over the rubber spirally. This provides very large contraction force but only at one direction. This paper considers 2 model combination consists from parametric and non-parametric model for practical and instant calibration instead of increasing number of parameter. The controller input is desired force:

$$p^* = g^{-1}(F_{PAM}^*; \mathcal{D}, \varepsilon) + f(F_{PAM}^*; \varepsilon; g_{err}^{-1}(\mathcal{D})), \quad (2)$$

where F_{PAM}^* is desired force of PAM ($F_{PAM}^* = \frac{\tau^*}{r_0}$), $f(\cdot)$ is non parametric model for the model error of $g_{err}^{-1}(\mathcal{D})$, p^* is the desired pressure as valve input, $g(\cdot)$ is PAM force parametric model from bladder pressure to muscle force, and $g^{-1}(\cdot)$ is inverse model of them with given contraction rate ε and calibration dataset \mathcal{D} . The asterisk (*) indicates desired value.

Although this model is provided at equilibrium point to ignore pressure dynamics, we include the Bowden cable hysteresis to consider its velocity.

A. Compensating Bowden Cable Friction

Bowden cables have considerable force transmission losses. We expand the friction coefficient model of static [22] to continuous. The static model can be written as

$$F = F_+ \exp(\mu\psi) \quad (0 < v), \quad (3)$$

where F_+ is the applied force and F is the force after loss. If the movement direction alters, the force loss relation is opposite. Switching two models generate discontinuity at zero velocity. We expand this model to a continuous definition using a sigmoid function $\sigma(v; \alpha) = \frac{1}{1 - \exp(-\alpha v)}$

$$F'^* = q(F^*; \mu, \alpha) = F^* [1 - (2\sigma(v; \alpha) - 1) \exp(\mu\psi)], \quad (4)$$

where F'^* is the compensated controller input for PAM force discussed above, v is velocity of the wire estimated from a joint encoder, and α is gain of sigmoid function. Increasing alpha decreases non-sensitive range to angle velocity. The compensated torque is same as original torque if angle velocity is zero.

B. PAM force model

The PAM force generation is process of pressure to contraction force conversion. The basic model-based force generation is described in literature [23], [24] as a 2nd order polynomial function at the equilibrium point. The parameters are provided conversion from PAM diameter and the angle of the embedded spiral-wire at the atmosphere pressure. In large force operations, we have to consider also inner wire extension and mechanical deformation. Here we consider Tendon-spring model for original PEHA system proposed in our previous work [15]. Consequently, the parameters are five valuables ($\lambda = (a, b, c, k, \varepsilon_0)$); (a, b, c) for the PAM nonlinearity and (k, ε_0) for inherent stiffness and initial slack of inner the wire. These parameters are calibrated in the system identification phase.

Thanks to Tendon-spring model, the inverse model can estimate dataset distribution with small number of parameter. However, there would be still remaining error that affect the torque controller. To our best knowledge, there is no theoretical model to support these errors and successful conventional approaches using heuristic non-linear model [21] or Neural Network [25]. Increasing the number of function parameters may require larger variational calibration dataset and may cause over fitting. We, thus, insist on using the theoretical parametric model to avoid the risk. Instead, we consider the error fitted by Sparse Pseudo-input Gaussian Process (SPGPs) [26]. Although Gaussian Process is a strong framework with Bayesian probabilistic model in behind to fit noisy sensor data, the computational cost is high; $\mathcal{O}(N)$ for the predictive mean estimation. After several pre-computation, SPGPs can reduces this cost to $\mathcal{O}(M)$ using sparse M pairs of pseudo-inputs $\bar{\mathbf{x}}_m$ and pseudo-target \bar{f}_m ($M \ll N$)

$$f(x) = \sum_m \alpha_m k(x; \bar{\mathbf{x}}_m, \bar{f}_m), \quad (5)$$

where x is two dimensional single point input of current state $x = (\varepsilon, F)$. Note that the pseudo pair of (\bar{x}_m, \bar{f}_m) corresponds to pseudo-input and pseudo pressure error. Hyper parameters are decided by Automatic Relevance Determination (ARD) [26].

V. EXPERIMENTS

A. PAM calibration

Fig. 8 shows the instance of the calibration dataset used for the upper PAM (40 mm) at EFE. 5 parameters of the PAM parametric inverse model are optimized from this experiment within the dataset respect to the error of the pressure using Levenberg–Marquardt algorithm. The forces are measured by well calibrated load cells. The best parameter was selected among 300 trials from random initialized parameter. The rest of the error is modeled by a nonparametric way using SPGPs.

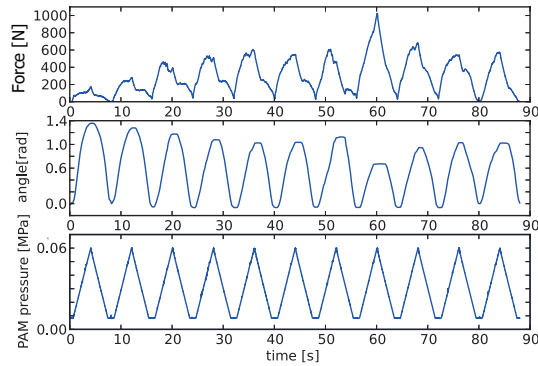


Fig. 8. The data set example for PAM calibration: triangle wave has sent to upper-body arm and the angle and the load cell reading were preserved at 250Hz sampling.

B. Torque based control: Gravity compensation and sensory based torque input

To compensate gravity force, the joint torque that corresponds to vertical assistive force against gravity is generated as:

$$\tau = \mathbf{J}^T \mathbf{G}_{\mathbf{r}+\mathbf{h}}, \quad (6)$$

where \mathbf{J} is the COM Jacobian matrix, $\mathbf{G}_{\mathbf{r}+\mathbf{h}}$ is the desired virtual forces, and τ is the desired torque at each joint of the exoskeleton robot. We validate the feed-forward torque controller for this task if the joint angle is kept when the operator moves and releases the system. Note that we did not use any position feedback.

Fig. 10 (a) shows the experiment setup for upper limb exoskeleton prototype. The mannequin arm with a free elbow joint was equipped on the exoskeleton arm, fasten by stretchable belts, and a flexible electro-goniometer (Biometrics Ltd.) was attached to the subject elbow joint for measurement.

Fig. 10 (b) demonstrates the gravity compensation task both for the robot arm and the mannequin arm using shoulder/elbow flexion/extension. The snapshots show the exoskeleton/mannequin arm can be held at different postures,

and the operator can move the link very easily because gravity force was successfully compensated by the proposed torque controller.

In the multimedia attachment, we also demonstrate that the elbow joint via a replacement torque signal that is acquired using inverse dynamics and goniometer. We sampled the subject’s elbow joint using the attached goniometer by real-time process, sampled at 200 Hz. The estimated elbow joint torque, using a standard inverse dynamics with Butterworth low pass filter, was sent to the torque controller of exoskeleton’s elbow as an input signal. The shoulder was controlled in the same way as done in the first task, e.g., gravity compensation of the total arm COM (using DOF joint kinematic model). In both cases, the shoulder and the elbow joint are controlled. The wrist of two PAMs are controlled by a constant pressure (0.25[Mpa]), resulting in keeping the joint (WFE) with inherent compliance. In both demonstrations, the passive rotation joint of the wrist (WR) was restrained by a mechanical clamp.

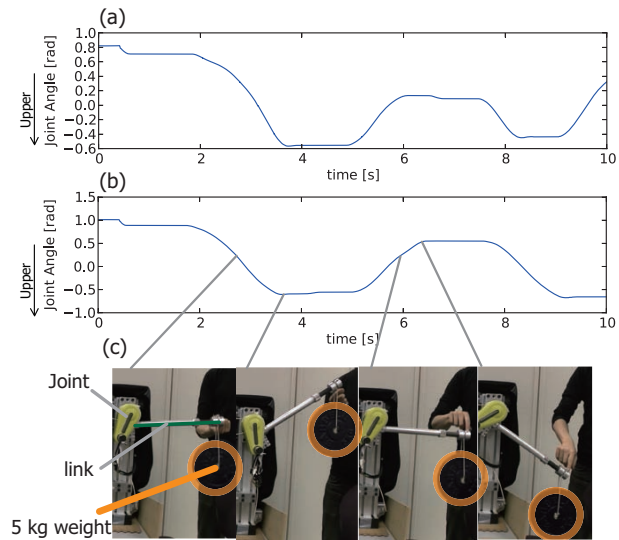


Fig. 9. Angle trajectories in gravity compensation task using One-DOF testing system: (a) 2.5kg weight gravity compensation task (b) 5.0kg weight gravity compensation task (c) Snapshots from 5.0 kg gravity compensation task

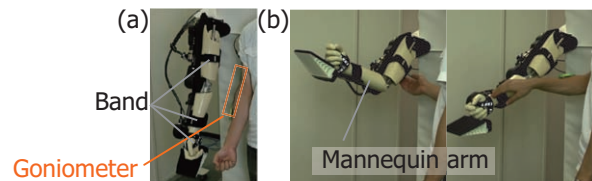


Fig. 10. Experimental setup for the arm exoskeleton: (a) A mannequin arm with passive elbow joint is attached to the upper limbs. The goniometer is attached to the subject elbow to conduct torque feedback control. (b) Two pictures demonstrate the exoskeleton with mannequin arm weight can be sustained at two different postures.

VI. CONCLUSIONS

In this paper, the challenges related to the development of the upper limb exoskeleton arm powered via pneumatic-

electric hybrid actuation with Bowden cables are described. Large torques are transmitted via Bowden cable from off-board Pneumatic Artificial Muscles (PAMs), combined with the small torque of the low-g geared motor that mechanically coupled within the joint. This approach can reduce the exoskeleton arm weight and the required space around the joint to address a multi degree of freedom design. The active joints of the prototyped exoskeleton arm are backdrivable with the capability of large torque generation using safe energy sources (pneumatic and small electric current). To control the joint using a torque controller, we considered a PAM force model with Tendon-spring under the equilibrium assumption that is combined with a Gaussian process. In the calibration phase, the parameters are calibrated from short term experiments to control PAM pressure based on torque input.

The gravity compensation task using both the One-DOF testing system and the prototyped exoskeleton arm demonstrated the backdrivable joint with large torque generation. We also show that the active movement using an electrogoniometer, the estimated joint torque of elbow angle with the standard inverse model was used as an input for the torque controller to move the exoskeleton elbow joint equipped with a mannequin arm. While further study is feasible to investigate the torque bandwidth of the hybrid approach, the implementation provided practical performance for the assistive applications.

As a future work, we consider developing the full upper body exoskeleton based on this mechanical design and the controllers.

VII. ACKNOWLEDGMENT

We thank Nao Nakano, Jun-ichiro Furukawa, and Akihide Inano for hardware maintenances and helping our experiments. This research was supported by a contract with the Ministry of Internal Affairs and Communications entitled, "Novel and innovative R&D making use of brain structures", and SRPBS by the MEXT. T.N. was partially supported by JSPS KAKENHI (#24700203). J.M. was partially supported by MEXT KAKENHI (#23120004). A part of this research was supported by Strategic International Cooperative Program, JST, JSPS and MIZS: Japan-Slovenia research Cooperative Program, and MIC-SCOPE.

REFERENCES

- [1] S. Jacobsen, "On the Development of XOS, a Powerful Exoskeletal Robot," in *2007 IEEE/RSJ International Conference on Intelligent Robots and Systems, Plenary Talk*, 2007.
- [2] H. Kazerooni, A. Chu, and R. Steger, "That Which Does Not Stabilize, Will Only Make Us Stronger," *International Journal of Robotics Research*, vol. 26, no. 1, pp. 75–89, 2007.
- [3] K. Suzuki, M. G. Kawamoto, H. Hasegarwa, and Y. Sankai, "Intension-based walking support for paraplegia patients with Robot Suit HAL," *Advanced Robotics*, vol. 21, no. 12, pp. 1441–1469, 2007.
- [4] S. K. Au, P. Dilworth, and H. Herr, "An ankle-foot emulation system for the study of human walking biomechanics," in *IEEE International Conference on Robotics and Automation*, 2006, pp. 2939–2945.
- [5] H. Kobayashi, A. Takamitsu, and T. Hashimoto, "Muscle Suit Development and Factory Application," *International Journal of Automation Technology*, vol. 3, no. 6, pp. 709–715, 2009.
- [6] G. Yamamoto and S. Toyama, "Development of Wearable-Agri-Robot-Mechanism for Agricultural Work," in *IEEE/RSJ International Conference on Intelligent Robots and Systems*, 2009, pp. 5801–5806.
- [7] T. Kagawa and Y. Uno, "Gait pattern generation for a power-assist device of paraplegic gait," in *The 18th IEEE International Symposium on Robot and Human Interactive Communication*, 2009, pp. 633–638.
- [8] R. Ham, T. Sugar, B. Vanderborght, K. Hollander, and D. Lefeber, "Compliant actuator designs," *IEEE Robotics and Automation Magazine*, vol. 16, no. 3, pp. 81–94.
- [9] J. F. Veneman, "A Series Elastic- and Bowden-Cable-Based Actuation System for Use as Torque Actuator in Exoskeleton-Type Robots," *The International Journal of Robotics Research*, vol. 25, no. 3, pp. 261–281, Mar. 2006.
- [10] H. Vallery, J. Veneman, E. van Asseldonk, R. Ekkelenkamp, M. Buss, and H. van Der Kooij, "Compliant actuation of rehabilitation robots," *IEEE Robotics and Automation Magazine*, vol. 15, no. 3, pp. 60–69.
- [11] D. Caldwell, N. Tsagarakis, S. Kousidou, N. Costa, and I. Sarakoglou, "'soft' exoskeletons for upper and lower body rehabilitation-design, control and testing," *International Journal of Humanoid Robotics*, vol. 04, no. 03, pp. 549–573, 2007.
- [12] J. F. Veneman, R. Kruidhof, E. E. G. Hekman, R. Ekkelenkamp, E. H. F. Van Asseldonk, and H. van der Kooij, "Design and Evaluation of the LOPES Exoskeleton Robot for Interactive Gait Rehabilitation," *IEEE Trans. Neural Syst. Rehabil. Eng.*, vol. 15, no. 3, pp. 379–386.
- [13] K. Kiguchi, "Active Exoskeletons for Upper-limb Motion Assist," pp. 1–18, Oct. 2007.
- [14] S.-H. Hyon, J. Morimoto, T. Matsubara, T. Noda, and M. Kawato, "Xor: Hybrid drive exoskeleton robot that can balance," in *Intelligent Robots and Systems (IROS), 2011 IEEE/RSJ International Conference on*. IEEE, 2011, pp. 3975–3981.
- [15] T. Noda, N. Sugimoto, J. Furukawa, M. Sato, S. Hyon, and J. Morimoto, "Brain-controlled exoskeleton robot for bmi rehabilitation," *Proceedings of IEEE-RAS International Conference on Humanoids (Humanoids)*, 2012.
- [16] T. Matsubara, T. Noda, S.-H. Hyon, and J. Morimoto, "An optimal control approach for hybrid actuator system," in *Humanoid Robots (Humanoids), 2011 11th IEEE-RAS International Conference on*. IEEE, 2011, pp. 300–305.
- [17] T. Teramae, T. Noda, S.-H. Hyon, and J. Morimoto, "Modeling and control of a pneumatic-electric hybrid system," in *Intelligent Robots and Systems (IROS), 2013 IEEE/RSJ International Conference on*. IEEE, 2013, pp. 4887–4892.
- [18] H. Higo, Y. Sakurai, T. Nakada, K. Tanaka, and K. Nagayama, "Dynamic characteristic and power consumption on an electro-pneumatic hybrid positioning system," *Proceedings of the 6th JFPS International*, vol. 2, p. 4, 2005.
- [19] I. Sardellitti, J. Park, D. Shin, and O. Khatib, "Air muscle controller design in the distributed macro-mini actuation approach," in *Intelligent Robots and Systems, 2007. IROS 2007. IEEE/RSJ International Conference on*. IEEE, 2007, pp. 1822–1827.
- [20] M. Kouchi and M. Mochimaru, "Aist research information database (<http://riodb.ibase.aist.go.jp/riohomee.html>)," *H16PRO287*, 2005.
- [21] A. Hildebrandt, O. Sawodny, R. Neumann, and A. Hartmann, "Cascaded control concept of a robot with two degrees of freedom driven by four artificial pneumatic muscle actuators," pp. 680–685, 2005.
- [22] L. E. Carlson, B. D. Veatch, and D. D. Frey, "Efficiency of Prosthetic Cable and Housing," *JPO: Journal of Prosthetics and Orthotics*, vol. 7, no. 3, p. 96, 1995.
- [23] K. Inoue, "Rubbertuators and applications for robots," in *Proceedings of the 4th international symposium on Robotics Research*. MIT Press, 1988, pp. 57–63.
- [24] D. Caldwell, A. Razak, and M. Goodwin, "Braided pneumatic muscle actuators," in *Proceedings of the IFAC Conference on Intelligent Autonomous Vehicles*, 1993, pp. 507–512.
- [25] K. K. Ahn and H. P. H. Anh, "Comparative study of modeling and identification of the pneumatic artificial muscle (PAM) manipulator using recurrent neural networks," *J Mech Sci Technol*, vol. 22, no. 7, pp. 1287–1298, Oct. 2008.
- [26] E. Snelson and Z. Ghahramani, "Sparse gaussian processes using pseudo-inputs," in *Advances in Neural Information Processing Systems 18*. MIT press, 2006, pp. 1257–1264.